

MASSIVELY PARALLEL SIMULATION OF PRODUCTION FROM FIELD-SCALE OCEANIC GAS HYDRATE DEPOSITS

Matthew T. Reagan, George J. Moridis, Katie L. Boyle, Craig M. Freeman,
Lehua Pan, Noel D. Keen, Jarle Husebo

Lawrence Berkeley National Laboratory
1 Cyclotron Rd.
Berkeley, CA 94720, USA
e-mail: mtreagan@lbl.gov

ABSTRACT

The quantity of hydrocarbon gases trapped in natural hydrate accumulations is enormous, leading to significant interest in the evaluation of their potential as an energy source. It has been shown that large volumes of gas can be readily produced at high rates for long times from some types of methane hydrate accumulations, by means of depressurization-induced dissociation, and by using conventional horizontal or vertical well configurations. However, these resources are currently assessed using simplified or reduced-scale 3D or 2D production simulations. In this study, we use the massively parallel TOUGH+HYDRATE code (pT+H) to assess the production potential of a large, deep-ocean hydrate reservoir and develop strategies for effective production. The simulations model a full 3D system of over a 38 km² extent, exploring the productivity of vertical and horizontal wells, single or multiple wells, and the variations in reservoir properties. Meshes involving up to 2.5M gridblocks, running on thousands of supercomputing nodes, are required to simulate such large systems at the highest level of detail. The simulations reveal the challenges inherent in producing from deep, relatively cold systems with extensive water-bearing channels and connectivity to large aquifers—mainly the difficulty of achieving depressurization and the problem of enormous water production. Also highlighted are new frontiers in large-scale reservoir simulation of coupled flow, transport, thermodynamics, and phase behavior, including the construction of large meshes and the computational scaling of larger systems.

INTRODUCTION

Gas hydrates are solid crystalline compounds in which gas molecules occupy the lattices of ice-like crystal structures called hosts (Sloan and Koh, 2008). They may occur in two distinctly different geographic settings, in the permafrost and in deep ocean sediments, where the necessary conditions of low T and high P exist for their formation and stability. The majority of these naturally occurring hydrates contain CH₄ in overwhelming abundance. Interest in hydrates is enhanced by ever-increasing global energy demand and the environmental desirability of natural gas. Although there has been limited work mapping and evaluating this resource on a global scale (Moridis et al., 2009), current estimates of in-place volumes vary widely (ranging between 10¹⁵ to 10¹⁷ ST m³), but the consensus is that the worldwide quantity of hydrocarbon gas hydrates is vast (Milkov, 2004; Klauda and Sandler, 2005; Burwicz et al., 2011). Even if only a small fraction of the most conservative estimate is recoverable, the sheer size of the resource is so large that it demands evaluation as a potential energy source.

However, not all hydrates are desirable targets for production (Moridis et al., 2011). Of the three possible methods of hydrate dissociation (Makogon, 1997) for gas production—depressurization, thermal stimulation, and use of inhibitors—depressurization appears to be the most efficient (Moridis et al., 2009). Recent studies (Moridis and Reagan, 2007a; b) have indicated that, under certain conditions, gas can be produced from natural hydrate deposits at high rates over long periods using conventional technology. Earlier work focused on production from vertical wells, but more recent studies (Moridis et al., 2008) show that horizontal wells

are more productive, and easier to manage, than vertical wells, if the technology is available.

The objective of this study is to simulate a realistic, 3D gas hydrate reservoir, using real geophysical data at the field scale. Previous studies (Moridis et al., 2009; 2011) have tended to focus on simple 2D modeling, 2D modeling with limited heterogeneity, or extremely simplified 3D modeling. Through a collaboration with Statoil, we were able to access real data on the geometry and geology of a known oceanic hydrate system that has been considered for commercial exploitation. Due to confidentiality agreements, the location of this deposit cannot be published, but the knowledge gained from this simulation work can be generally applied, and used to evaluate any kind of oceanic deposit. The deposit, illustrated in Figure 1, is an oceanic, layered system, approximately 7 km×5.5 km×350 m thickness. The hydrate is arranged in high-permeability “channels” bounded by slightly lower-permeability “levees.” The system is likely impermeable at the top and bottom boundaries, but may connect to an aquifer along the *x-z* face. Note, via the slicing plane, the layering of the hydrate-bearing channels.

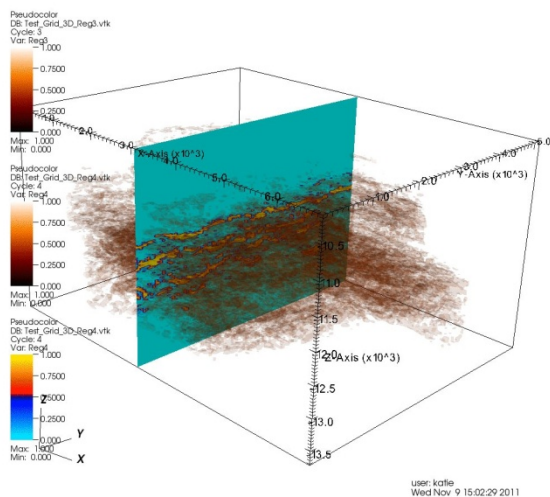


Figure 1. Illustration of the location of hydrate layers within the reservoir domain.

METHODOLOGY

Simulators

Due to the computational challenges of simulating a field-scale system, we use the MPI-parallel TOUGH+HYDRATE code (pT+H) (Zhang et al., 2008). pT+H contains the same coupled thermal-hydrological-chemical capabilities of serial TOUGH+HYDRATE v1.1 (Moridis et al., 2008), but can be executed on shared- or distributed-memory clusters using standard OpenMPI libraries (<http://www.openmpi.org/>).

Mesh Generation

The construction of 3D volume meshes for systems of this scale is well beyond the means of the standard TOUGH+ MeshMaker routine. Therefore, we deploy advanced tools.

For vertical-well scenarios, the grid was generated using WinGridder (Pan, 2008), an interactive application developed for the Yucca Mountain project. The initial vertical well configuration involves a roughly rectilinear, layer-by-layer mesh of the reservoir, as taken directly from the Statoil dataset, with the discretization matching that of the geophysical data. A cylindrical mesh, with a center at the well, was placed through the region of greatest hydrate accumulation, with the two meshes interpolated at the boundary to conform to TOUGH element-connection rules. The vertical-well mesh is illustrated in Figure 2.

Note in the figure that the domain has been trimmed, with regions of the mesh that do not represent permeable reservoir rocks removed to promote computational efficiency. All subsequent meshing begins with this “reduced” mesh, which contains 1,663,900 elements.

WinGridder does not have the ability to interpolate a horizontal near-well zone into a roughly rectilinear mesh. Therefore, to build the horizontal-well system, a combination of custom tools for manipulating the raw list of element centroids and creating new mesh-element configurations (i.e., cylinders) is combined with the meshing toolkit Voro++ (Rycroft, 2009). Voro++ is a C++ library capable of generating a fully-3D Voronoi mesh for any valid configura-

tion of cell centers. The Voro++ library keeps track of all relevant cell and interface properties and makes them available for manipulation. This allows the creation of highly flexible and dynamically refined meshes.

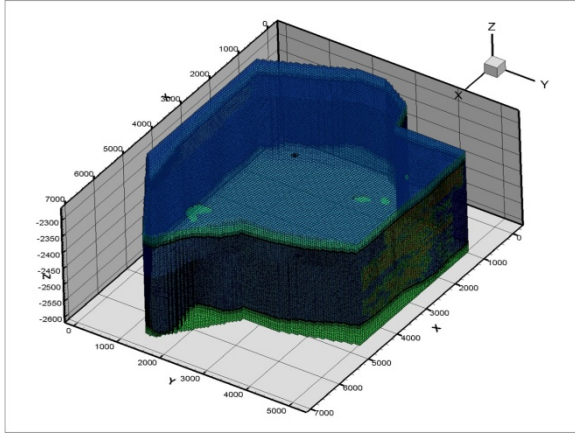


Figure 2. Illustration of the 3D finite-volume mesh, with trimmed boundaries, for the single vertical well scenario. The intersection of the cylindrical well-zone mesh with the top boundary can be seen in the center of the top surface.

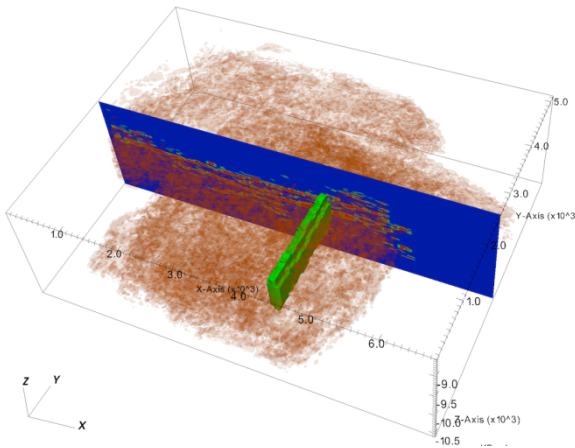


Figure 3. Diagram of the placement of the horizontal well and surrounding cylindrical mesh. Hydrate-bearing sediments are plotted as brown volumes.

For the horizontal well, the geophysical data was analyzed to locate the longest continuous horizontal layers of hydrate more than 60 m thick. A region of roughly 65 m thickness was located near the core of the system, accommo-

dating a horizontal well 1,900 m in length, with no intersection with non-hydrate bearing channels or levees. A cylindrical mesh was constructed around the well to a radius of 250 m, and this radial mesh was inserted into the rectilinear mesh derived from the geophysical data (Figure 3). Element properties (i.e., hydrate saturation) were interpolated from the rectilinear data onto the new mixed mesh. The resulting mesh contains 2,264,000 elements, requiring the simultaneous solution of over 9,000,000 equations, making this the largest TOUGH simulation ever attempted.

Not surprisingly, meshes of this size are challenging to manipulate. Perl and python-based scripts were developed to edit the MESH files after generation (because they are too large for most fully graphical text editors). The system was brought first to hydrostatic equilibrium at the known depth (proprietary) and then to thermal equilibrium using the known geothermal gradient. Due to the size and extent of the system, this consumed significant computing time. Hydrate was added to the system according to the distribution derived from the geophysical data. The system was then allowed to reach full thermal, hydrological, and chemical equilibrium at stated conditions before any simulations were performed.

Reservoir Properties

Although full details of the system may not be disclosed, the initial set of reservoir properties is shown in Table 1.

Table 1. Reservoir parameters.

| Region | k (mD) | ϕ | S_H | S_W |
|--------------|----------|--------|-------|-------|
| 0. Bound | 0 | 0.0 | 0.0 | 1.0 |
| 1. Levee 1 | 100 | 0.2 | 0.0 | 1.0 |
| 2. Levee 2 | 100 | 0.21 | 0.0 | 1.0 |
| 3. Levee 3 | 100 | 0.22 | 0.7 | 0.3 |
| 4. Channel 1 | 10000 | 0.33 | 0.7 | 0.3 |
| 5. Channel 2 | 10000 | 0.34 | 0.0 | 1.0 |
| 6. Channel 3 | 10000 | 0.35 | 0.0 | 1.0 |

Regions 3 and 4 are the hydrate-bearing media seen in Figures 1 and 3. Geophysical data suggested the presence of free gas in the reservoir, but TOUGH+HYDRATE pre-run thermo-

dynamic consistency checks ruled this as impossible under the stated conditions. Therefore, the gas was removed from the model.

For additional parameters, we used data from one of the few well-characterized reservoir-grade oceanic hydrate deposits, the Tigershark deposit (Moridis and Reagan, 2007a,b). Relative permeability exponents were estimated by fitting to Statoil effective permeability data. The pressure specified at the well was selected to be 3.0 MPa to prevent ice formation in the wellbore. Other details about Tigershark, the configuration of the simulated wellbore, and examples of production from such a system, can be found in Moridis and Reagan (2007a,b). Key simulation parameters are provided in Table 2.

Table 2. Other simulation parameters.

| | |
|--|---|
| Water salinity (mass fraction) | 0.035 |
| Grain density r_R (all formations) | 2750 kg/m ³ |
| Constant pressure at the well P_w | 3.0 x 10 ⁶ Pa |
| Dry thermal conductivity k_{QRD} (all formations) | 0.5 W/m/K |
| Wet thermal conductivity k_{QRW} (all formations) | 3.1 W/m/K |
| Composite thermal conductivity model (Moridis et al., 2008) | $\frac{k_{QC} = k_{QRD}}{+(S_A^{1/2} + S_H^{1/2})(k_{QRW} - k_{QRD}) + f S_I k_{QI}}$ |
| Capillary pressure model (van-Genuchten, 1980; Moridis et al., 2008) | $P_{cap} = -P_0 \left[(S^*)^{-1/\lambda} - 1 \right]^{-\lambda}$ |
| S_{irA} | 1 |
| λ | 0.77 |
| P_{max} | 10 ⁶ Pa |
| Relative permeability | $k_{rA} = (S_A^*)^n$ |
| Model (Moridis et al., 2008) | $k_{rG} = (S_G^*)^n$ |
| | $S_A^* = (S_A - S_{irA}) / (1 - S_{irA})$ |
| | $S_G^* = (S_G - S_{irG}) / (1 - S_{irA})$ |
| | OPM model |
| n (fitted from data) | 4.4292 |
| S_{irG} | 0.02 |
| S_{irA} | 0.20 |

RESULTS AND DISCUSSION

Production from a Vertical Well

Initial simulation work by Statoil, using the CMG-STARs with gas hydrate add-ons, suggested that the system could be productive if vertical wells were drilled into the lower part of the formation near areas of high hydrate saturation. However, these simulations used a 2D slice of the full system and assumed significant free gas in the initial configuration of the reservoir. In contrast, here we begin by simulating production from the 3D, single vertical well shown in Figure 2.

We simulate three well configurations: (1) a well perforated throughout the entire hydrate-bearing zone (“Long”), (2) a well perforated only within the topmost hydrate layer (“Short”), and (3) a well perforated within the topmost layer, with the impermeable system boundaries brought inward to simulate the well as part of 500 m well spacing pattern (no-flow boundaries 250 m from the well). We also estimate sensitivity to system permeability by performing four additional simulations in the 500 m pattern case: reducing the permeability of the non-hydrate-bearing levees to 100 mD, 10 mD, 1 mD, and 0.01 mD. For each case, we simulate up to three years of constant-pressure production, using 200–220 processors with pT+H on a departmental computing cluster.

Comparison of Vertical Well Configurations

Figures 4 and 5 track the evolution of production for the seven cases. In Figure 4, we see the hydrate dissociation (“release”) begins immediately for the long-interval case, but quickly subsides. Producing from a small interval within the top layer of hydrate (“short”), results in far less dissociation, and no sign of strong methane release. However, if this short-interval well is producing as part of a 500 m pattern, we see strong dissociation/methane release after 1.5 years of depressurization for all subsequent scenarios, with lower-permeability levees surrounding the hydrate, resulting in earlier dissociation of hydrate.

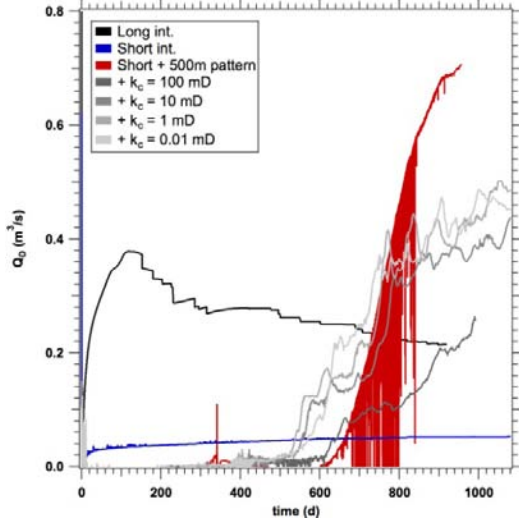


Figure 4. Rate of hydrate dissociation, Q_D , for the reservoir as a whole, for the vertical well scenarios.

Figure 5 shows the resulting methane production at the well for the various scenarios. The full interval generates the highest rates of methane production (unsurprising at first, due to the much greater extent and penetration of the perforated interval), with other configurations lagging significantly. However, production via the long interval levels off quickly, and does not achieve commercially viable rates within 3 yr. Among the other methods, wells in a 500 m pattern with low-permeability levees show some gains in production rate after 2.5 yr, but the viability of these methods are questionable.

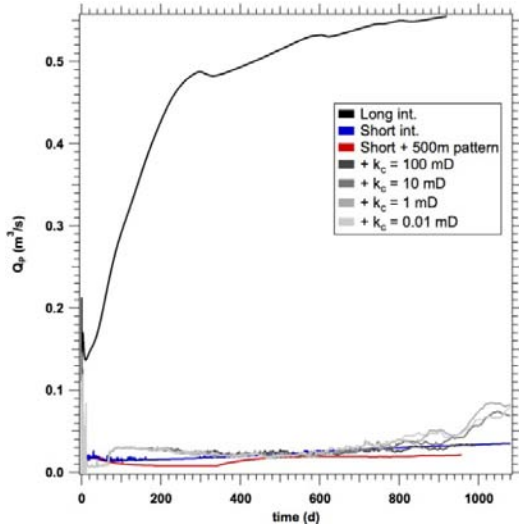


Figure 5. Rate of methane production at the well, Q_P , for the vertical well scenarios.

The nature of the problem is worse than initially suspected, however, for reasons shown by Figure 6, which shows the amount of water removed per m^3 of methane produced, reported as cumulative quantities vs. time. In each case, we see that massive amounts of water are moved to achieve small rates of dissociation and production, even for cases where the communicating water-filled levees have extremely reduced permeability. In absolute quantities, the “best case” scenario produces 4×10^8 kg of water over 3 yr, and the full interval would require the removal of a colossal 10^{11} kg of water in 2.5 yr—nearly one tonne per second.

At best, we also see that 200 kg of water is removed per m^3 of methane after 3 yr, a value that is suspiciously close to the solubility of methane in water under reservoir conditions. This suggests that mobile free gas is not being produced in significant quantities via depressurization, and that the bulk of produced methane results from dissolution of methane directly from solid hydrate and transport to the well via the aqueous phase.

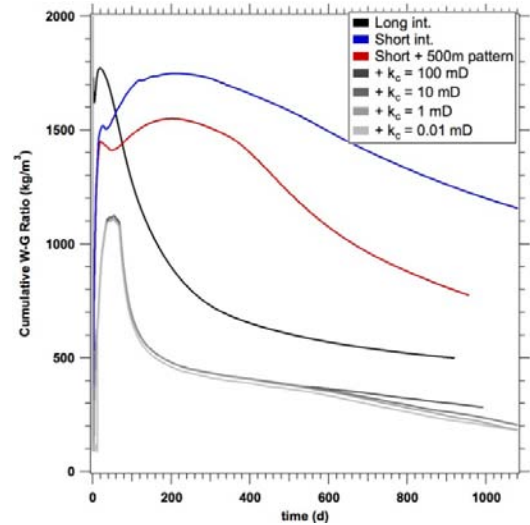


Figure 6. Ratio of total water production to total methane production (cumulative at time t) for the vertical well scenarios.

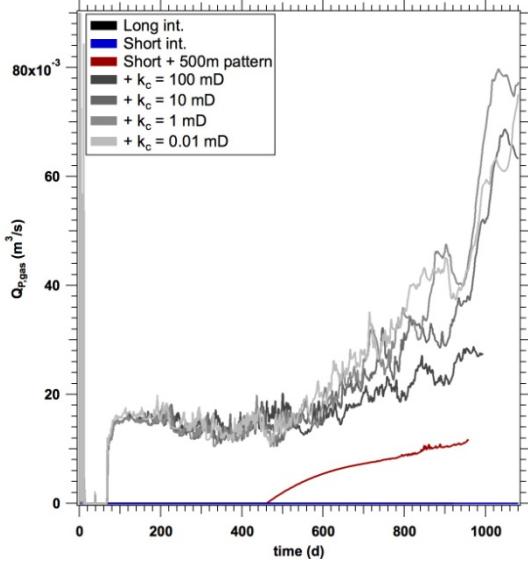


Figure 7. Rate of methane production at the well in the gas phase, $Q_{p,gas}$, for the vertical well scenarios.

Figure 7, showing only production of methane in the gas phase excluding aqueous transport, confirms this problem. Only wells in a 500 m pattern produce any gas at all, and even in those cases, the production of free gas is orders of magnitude less than gas transport in the aqueous phase. It is clear that the presence of large amounts of water in this hydrate reservoir hampers effective depressurization and dissociation. This effect has been seen clearly before, where simulations of Class 2 systems strongly suggest that impermeable boundaries are crucial (Moridis et al., 2009).

Production from a Horizontal Well

For Class 2 and Class 3 hydrate deposits, it has been demonstrated that horizontal wells, properly located, are a far more effective production strategy (Moridis et al., 2008). Therefore, we simulate production from the horizontal well shown in Figure 3, with all simulation and reservoir parameters otherwise unchanged from the vertical-well cases. However, due to the larger mesh (2.46M vs. 1.66M gridblocks) and the nature of the Voronoi grid (on average, more connections per element), the computational requirements for this simulation are approximately an order of magnitude greater. Initial equilibration was performed using our 220-processor in-house cluster, but production was scaled up to the

“Hopper” supercomputer, part of NERSC, for multi-day runs using 960 and 1,920 processors. To date, we have been able to simulate 135 days of production time, with simulations ongoing.

Evolution of the rate of hydrate dissociation/methane release (Q_R) and the rate of methane production at the well (Q_P) are provided in Figure 8. Unlike the vertical well examples, here we see that release exceeds production from the beginning, which is necessary to generate free gas in the reservoir for later production (Moridis and Reagan, 2007a;b). Water production (Q_W) is large but steady, and comparable to the best-case vertical well scenario (with greater access to the reservoir via a single well). However, after less than 5 months of production, we see that both release and production are ceasing to increase with time, while water production remains roughly constant. This suggests that once again, effective depressurization is being hindered by the inflow of large quantities of water from the surrounding formation. As economically viable production rates for offshore wells need to reach orders of millions of cubic feet per day (10^4 – 10^5 m³/day), this system does not appear to be a desirable production target.

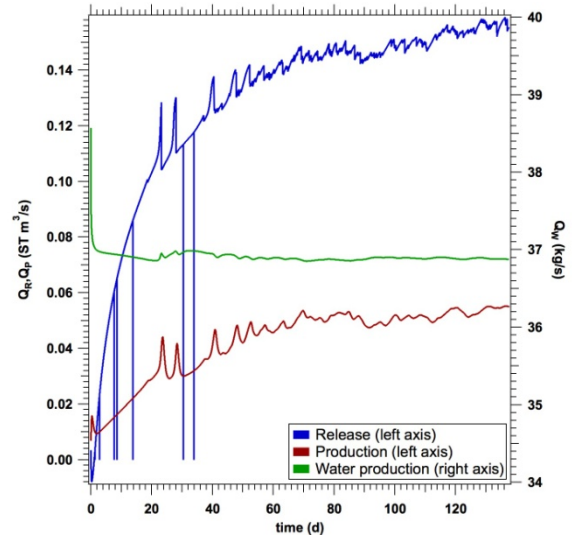


Figure 8. Rate of hydrate dissociation and methane release (Q_R), rate of methane production at the well (Q_P), and rate of water production at the well (Q_W , right axis) for the horizontal well scenario.

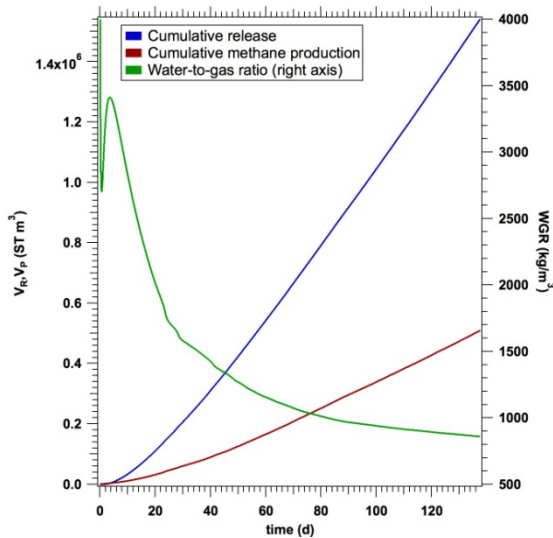


Figure 9. Cumulative methane release (V_R), cumulative methane production (V_P), and ratio of total water production to total methane production (V_W , right axis), for the horizontal well scenario.

Cumulative quantities of methane, released and produced, are shown in Figure 9. More significant, however, is the water-to-gas ratio, shown in green. While this ratio drops rapidly as production proceeds, the curve is heading toward asymptotic behavior at values of 700 to 800 kg per m^3 , which suggests again that transport of methane is entirely in the aqueous phase, and even then, that the quantity of water produced greatly exceeds that quantity of water needed to dissolve and transport the methane seen at the well. It is therefore likely that the hydrate zone around the well has been perforated by dissociation, connecting the well to the gigantic reservoir of mobile water surrounding the hydrate layers and hindering depressurization after over a few months of production.

CONCLUSIONS

This study has been the first 3D simulation, at this scale, of production in a real, field-scale oceanic hydrate reservoir. While the simulations use the most extensive, realistic, and data-based model to date, the insights found here strongly relate to earlier studies on the productivity and non-productivity of various configurations of hydrates.

Earlier work has strongly suggested that impermeable boundaries (i.e., sufficiently impermeable to allow strong depressurization of the reservoir through conventional technology) are the key to efficient and economical production (Moridis and Reagan, 2007a;b; Moridis et al., 2009;2011). While this reservoir (as modeled) is indeed bounded on a large scale, the layers of high-saturation hydrate are adjacent to, and effectively surrounded by, levees and channels of high-permeability, water-saturated media. Even when those levees are reduced in permeability, creating bounded, Class 2 systems, the sheer quantity of available water makes depressurization difficult on a reservoir scale or even on a local scale, assuming a pattern of wells and short perforation intervals.

Previous work determined that a horizontal well, properly placed, can mitigate some of these problems as long as the horizontal well stays within the hydrate layer and does not connect to surrounding water-filled media. Our early results for this configuration show that large quantities of water are able to reach the well early in the depressurization process, reducing depressurization effectiveness. Whether this is due to rapid dissociation and breakthrough, or other effects (for example, the greatly reduced but still finite effective permeability of hydrate-bearing media) remains to be proven—ongoing simulations will produce detailed 3D images of system evolution to evaluate this hypothesis. As a result, it is becoming clear that systems with large quantities of water in communication with the hydrate reservoir, even if not connection to aquifers beyond reservoir boundaries, are particularly challenging production targets. Permeability of the bounding media, as well as distance from the hydrate stability boundary and configuration of the hydrate into large contiguous masses, needs to be considered in reservoir evaluation.

It is somewhat disappointing that simulations of this size and scale result in “lackluster” results—in terms of active hydrate dissociation, gas formation, and the coupled thermodynamic and transport processes seen in more active and productive systems. However, it is important to note that these are the largest TOUGH simulations to date, with the simultaneous solution of 9,000,000 equations at each step, plus fully

described multiphase thermodynamics. The simulations show that mesh complexity becomes critical for large systems, as the “layered” and mainly rectilinear vertical well mesh (1.66M elements) can be realistically run on a small departmental cluster, while the more complex Voronoi grid used in the horizontal well simulations (2.46M elements) may require over a million processor-hours of time to complete the assessment. The development of user-friendly meshing tools and perhaps active mesh refinement and de-refinement may be needed to move TOUGH simulations fully into the massively parallel universe, as the standard ASCII TOUGH+ hydrate MESH, INCON, and SAVE files quickly become too large to manipulate via hand-editing. Finally, the traditional TOUGH-family visualization methods, mainly via standard outputs or ASCII-based, Tecplot-formatted files, are insufficient to handle datasets of this size. Preliminary real-time visualization of pT+H using Visit (<https://wci.llnl.gov/codes/visit/>) has been successful, although the generation of publication-grade images has not yet been achieved. Key hurdles include finding and implementing modern data formats, and converting the nonstandard TOUGH finite-volume meshes into forms more compatible with high-performance visualization software. These problems must be solved through enhancements and modernization of the pT+H code base.

ACKNOWLEDGMENTS

This research was funded by Statoil Inc. This research used resources of the National Energy Research Scientific Computing Center, which is supported by the Office of Science of the U.S. Department of Energy under Contract No. DE-AC02-05CH11231. The authors would like to thank Shiv K. Pande for assistance with data visualization.

REFERENCES

Burwicz, E.B., Rupke, L.H., Wallmann, K., Estimation of the global amount of submarine gas hydrates formed via microbial methane formation based on numerical reaction-transport modeling and a novel parameterization of Holocene sedimentation.

Geochimica et Cosmochimica Acta, 75, 16, 4562-4576, 2011.

Klauda, J.B., Sandler, S.I., Global distribution of methane hydrate in ocean sediment. *Energy and Fuels*, 19, 459, 2005.

Makogon, Y.F. *Hydrates of Hydrocarbons*. Tulsa, OK: Penn Well Publishing Co., 1997.

Milkov, A.V. Global estimates of hydrate-bound gas in marine sediments: how much is really out there? *Earth Science Reviews*, 66, 183, 2004.

Moridis, G.J., Reagan, M.T. Gas Production From Oceanic Class 2 Hydrate Accumulations, OTC 18866, *Proc. 2007 Offshore Technology Conference*, Houston, Texas, U.S.A., 30 April–3 May 2007a.

Moridis, G.J., Reagan, M.T. Strategies for Gas Production From Oceanic Class 3 Hydrate Accumulations, OTC 18865, *Proc. 2007 Offshore Technology Conference*, Houston, Texas, 30 April – 3 May 2007b.

Moridis, G.J., M.B. Kowalsky, Pruess, K. TOUGH+HYDRATE v1.0 User’s Manual: A Code for the Simulation of System Behavior in Hydrate-Bearing Geologic Media, Report LBNL-0149E, Lawrence Berkeley National Laboratory, Berkeley, CA, 2008.

Moridis, G.J., Reagan, M.T., Zhang, K. The Use of Horizontal Wells in Gas Production from Hydrate Accumulations, *Proc. 6th International Conference on Gas Hydrates*, Vancouver, BC, July 6-10, 2008.

Moridis, G.J., Collett, T.S., Boswell, R., Kurihara, M., Reagan, M.T., Koh, C., Sloan, E.D. Toward Production From Gas Hydrates: Current Status, Assessment of Resources, and Simulation-Based Evaluation of Technology and Potential. SPE 114163, *SPE Journal*, 12(5), 745-771, 2009.

Moridis, G.J., Collett, T.S., Pooladi-Darwish, M., Hancock, S., Santamarina, C., Boswell, R., Kneafsey, T., Rutqvist, J., Kowalsky, M.J., Reagan, M.T., Sloan, E.D., Sum, A.K., and Koh, C., Challenges, Uncertainties and Issues Facing Gas Production From Hydrate Deposits in Geologic Systems, LBNL-4254E, *SPE Res. Eval. & Eng*, 14(1), 76-112, 2011.

- Pan, L., *User's Information for WinGridder V3.0.*, LBNL Report 273E, Lawrence Berkeley National Laboratory, Berkeley, CA, 2008.
- Rycroft, C.H., Voro++: A three-dimensional Voronoi cell library in C++, *Chaos*, 19, 041111 (2009).
- Sloan, E.D., and C. Koh, *Clathrate Hydrates of Natural Gases. 3rd Edition*, Taylor and Francis, Inc., Boca Raton, FL, 2008.
- van Genuchten. A Closed-Form Equation for Predicting the Hydraulic Conductivity of Unsaturated Soils. *Soil Sci. Soc.*, 44, 892, 1980.
- Zhang, K., Moridis, G.J., Wu, Y.S., Pruess, K. A domain decomposition approach for large-scale simulations of flow processes in hydrate-bearing geologic media. Proc. 6th International Conference on Gas Hydrates, Vancouver, BC, July 6-10, 2008.